Spectrochimica Acta Part A: Molecular and Biomolecular Spectroscopy 141 (2015) 233–238

Contents lists available at ScienceDirect

Spectrochimica Acta Part A: Molecular and Biomolecular Spectroscopy

journal homepage: www.elsevier.com/locate/saa

Synthesis, DFT calculations of structure, vibrational and thermal decomposition studies of the metal complex $Pb[Mn(C_3H_2O_4)_2(H_2O)_2]$

Diego M. Gil [a,*], Raúl E. Carbonio [b,1], María Inés Gómez [c,*]

[a] INQUINOA – CONICET, Instituto de Química Física, Facultad de Bioquímica, Química y Farmacia, Universidad Nacional de Tucumán, San Lorenzo 456, T4000CAN San Miguel de Tucumán, Argentina
[b] INFIQC – CONICET, Departamento de Físico Química, Facultad de Ciencias Químicas, Universidad Nacional de Córdoba, Ciudad Universitaria, X5000HUA Córdoba, Argentina
[c] Instituto de Química Inorgánica, Facultad de Bioquímica, Química y Farmacia, Universidad Nacional de Tucumán, Ayacucho 471, 4000 San Miguel de Tucumán, Argentina

HIGHLIGHTS

- The metallo-organic complex $Pb[Mn(C_3H_2O_4)_2(H_2O)_2]$ was synthesized and characterized.
- The complex crystallizes in the hexagonal crystal system, space group $P6_3/mcm$.
- The vibrational behavior of the complex $Pb[Mn(C_3H_2O_4)_2(H_2O)_2]$ was analyzed using IR and Raman spectroscopy.
- The thermal treatments of $Pb[Mn(C_3H_2O_4)_2(H_2O)_2]$ in air produce the mixed oxide Pb_2MnO_4 with PbO as impurity.

GRAPHICAL ABSTRACT

IR and Raman spectra of $Pb[Mn(C_3H_2O_4)_2(H_2O)_2]$ and the optimized molecular structure.

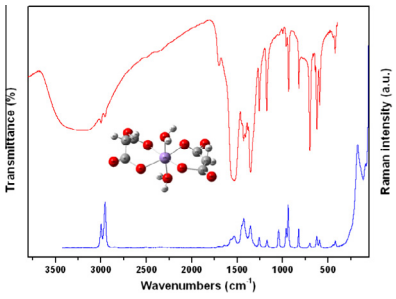

ARTICLE INFO

Article history:
Received 19 August 2014
Received in revised form 4 November 2014
Accepted 23 January 2015
Available online 3 February 2015

Keywords:
Metallo-organic complex
Thermal decomposition
IR and Raman spectroscopy
DFT calculations
Powder diffraction

ABSTRACT

The metallo-organic complex $Pb[Mn(C_3H_2O_4)_2(H_2O)_2]$ was synthesized and characterized by IR and Raman spectroscopy and powder X-ray diffraction methods. The cell parameters for the complex were determined from powder X-ray diffraction using the autoindexing program TREOR, and refined by the Le Bail method with the Fullprof program. A hexagonal unit cell was determined with $a = b = 13.8366(7)$ Å, $c = 9.1454(1)$ Å, $\gamma = 120°$. The DFT calculated geometry of the complex anion $[Mn(C_3H_2O_4)_2(H_2O)_2]^{2-}$ is very close to the experimental data reported for similar systems. The IR and Raman spectra and the thermal analysis of the complex indicate that only one type of water molecules is present in the structure. The thermal decomposition of $Pb[Mn(C_3H_2O_4)_2(H_2O)_2]$ at 700 °C in air produces PbO and Pb_2MnO_4 as final products. The crystal structure of the mixed oxide is very similar to that reported for Pb_3O_4.

Introduction

The structure and properties of heteronuclear complexes involving carboxylato-bridged ligands have been widely investigated for a long time because of their potential applications in molecular magnetic materials [1]. The malonato anion, with two neighboring carboxylate groups, is a very versatile ligand and it has been used for the synthesis of crystalline coordination materials of diverse architectures, as the result of its various potential binding

* Corresponding authors at: Instituto de Química Física, Facultad de Bioquímica, Química y Farmacia, Universidad Nacional de Tucumán, San Lorenzo 456, T4000CAN Tucumán, Argentina. Tel.: +54 381 4311044; fax: +54 381 4248169 (D.M. Gil). Instituto de Química Inorgánica, Facultad de Bioquímica, Química y Farmacia, Universidad Nacional de Tucumán, Ayacucho 471, 4000 San Miguel de Tucumán, Argentina. Tel.: +54 381 4247752x7069; fax: +54 381 4248169 (M.I. Gómez).
E-mail addresses: dmgil@fbqf.unt.edu.ar (D.M. Gil), mgomez@fbqf.unt.edu.ar (M.I. Gómez).
[1] Member of the Research Career of CONICET.

http://dx.doi.org/10.1016/j.saa.2015.01.057
1386-1425/

modes to transition metals as well as its participation in hydrogen bonding interactions [1–3]. The malonato ligand can simultaneously adopt monodentate, various bischelating coordination modes and different carboxylate bridging modes (*syn–syn*, *syn–anti* and *anti–anti*) giving rise to a variety of structures and being a useful tool to connect different metals and transmitting different magnetic interactions. In this way, ferromagnetically or anti-ferromagnetically coupled dimmers and alternating chains have been obtained [4–6].

The heteronuclear complexes of the type $A[M(C_3H_2O_4)_2(H_2O)_4]$ (A = alkaline earth metals; M = transition metals) were used as precursors for the synthesis of perovskite-type oxides [7–11]. The thermal decomposition of metallo-organic precursors allowed us to prepare metastable or stable phases at lower temperatures containing smaller grain sizes than those obtained from the ceramic method [7–11]. Using this method of synthesis, the diffusion distances between metal centers are remarkably reduced and, as a consequence, the reaction times and temperatures are reduced compared with other methods of synthesis. The obtained product presents more purity, being highly homogeneous and the grain size is considerably smaller [12–18]. Although different ligands can be used in the synthesis of these compounds [12–18], the carboxylate ligands have often been used to complex the transition metal ions. In this way, malonato is a good bridging ligand extensively used due to the facility to form polynuclear complexes.

In the present article we report the synthesis, structural and vibrational characterization of the heteronuclear complex $Pb[Mn(C_3H_2O_4)_2(H_2O)_2]$ and its thermal decomposition products. The cell parameters of the complex were obtained by the Le Bail method using conventional powder X-ray diffraction (PXRD) data. Theoretical calculations of the $[Mn(C_3H_2O_4)_2(H_2O)_2]^{2-}$ complex anion have been used to understand the structural characteristics of the metal complex. The thermal decomposition of the complex was evaluated by means of thermogravimetric (TG) and differential thermal (DT) analysis. IR and Raman spectroscopy measurements were performed in order to assign the modes of vibrations characteristics of the malonato ligand bounded to the metal centers. The thermal decomposition products were identified and characterized by IR spectroscopy and PXRD data.

Experimental

Synthesis of the complex $Pb[Mn(C_3H_2O_4)_2(H_2O)_2]$

Manganese (II) carbonate (1.0 mmol) suspended in 5 cm^3 of distilled water was allowed to react with malonic acid (2.5 mmol) in a steam bath. Solid sodium carbonate (2.5 mmol) was added to the resulting clear solution after dilution to 25 cm^3 with cold water. Once the effervescence is finished, the solution is filtered and lead (II) nitrate (1.0 mmol) dissolved in a minimum amount of water was added. The white resulting precipitate was filtered, washed many times with distilled water and ethanol, and finally stored in a dry box with silica gel (Yield 82%). Attempts to obtain single crystal for the title compound have been unsuccessful. The results of elemental analysis were consistent with the following stoichiometry: Calculated for $C_6H_8O_{10}PbMn$: C, 14.39; H, 1.59; O, 31.86%. Found: C, 14.68; H, 1.62; O, 31.92%.

The solid state properties of the obtained material were studied with laboratory PXRD, FTIR and Raman spectroscopy and thermogravimetric and differential thermal analysis.

Characterization

Elemental analysis (C, H, O) were carried out with a Carlo Erba 1108 analyzer. TG and DT curves were obtained in a Shimadzu TGA/DTA-50 in the temperature range 20–800 °C at heating rate of 5 °C/min under flowing air. The infrared (FTIR) spectrum of $Pb[Mn(C_3H_2O_4)_2(H_2O)_2]$ at room temperature (RT) was recorded in KBr pellets within 4000–400 cm^{-1} range using a Perkin Elmer GX1 FTIR instrument in the transmission mode. The Raman spectrum of the solid complex between 3500 and 50 cm^{-1} was measured on a Thermoscientific DXR Raman microscope. Data were collected using a diode-pump, solid state laser of 532 nm (5 cm^{-1} spectral resolution). A confocal aperture of 25 μm pinhole was used. A 10× objective was used when collecting Raman data. The sample was placed on gold-coated glass slide. In order to achieve a sufficient signal to noise ratio, 30 expositions with exposure time of 2 s were accumulated for the sample. The laser power was maintained at 10 mW when collecting data. Laboratory PXRD profiles for $Pb[Mn(C_3H_2O_4)_2(H_2O)_2]$ and the thermal decomposition products at different temperatures were obtained at RT in a PANalytical X'Pert Pro powder diffractometer with Cu Kα radiation, between 5° and 70° in 2θ steps of 0.02 and counting time of 1 s per step. The PXRD pattern was indexed with the autoindexing program TREOR [19]. The diffractogram was refined by the Le Bail method [20], with the Fullprof program [21]. A pseudo-Voigt function convoluted with an axial divergence asymmetry function [22] was chosen to generate the peak shapes. The following parameters were refined: zero-point, unit cell parameters, background points and profile parameters (U, V, W and X) and asymmetry parameters. The computational study of the $[Mn(C_3H_2O_4)_2(H_2O)_2]^{2-}$ complex anion was performed using the density functional theory (DFT) methods with the hybrid B3LYP [23–25] implemented in the Gaussian 03 program [26]. The IR and Raman spectra assignments were made from the calculation of the second derivates after full geometry optimization of the $[Mn(C_3H_2O_4)_2(H_2O)_2]^{2-}$ anion. The LANL2DZ basis set were used for the metal center and the 6-311G(d,p) for the non metal atoms.

Results and discussion

Thermal analysis

The thermal behavior of the $Pb[Mn(C_3H_2O_4)_2(H_2O)_2]$ was studied by means of TG and DT analysis. Fig. 1 shows TG-DTA curves from the thermal decomposition of the complex measured in flowing air. The examination of these curves indicates that all the transformations observed in the complex are associated with mass changes. The first step for the thermal decomposition finishes at 190 °C with a mass loss of 7.25%. This step is associated to the loss of two water molecules (theoretical value: 7.17%). The dehydration process takes place in only one step, suggesting that all of the water molecules are similar. The DT curve shows an endothermic peak located at 183 °C associated to the dehydration process. The following decomposition step occurs in the temperature range 200–350 °C with an experimental mass loss of 23.42% which is attributed to the decarboxylation of two malonato ligands (theoretical value, 22.30%). The DT curve shows two exothermic peaks located at 267 and 301 °C indicating that the decarboxylation of the ligand occurs in two steps. The third decomposition step finishes at 500 °C and it corresponds to the decomposition of $PbCO_3$ with formation of PbO. $PbCO_3$ is formed by reaction of CO_2 formed during the decarboxylation of the ligand. According to the results reported by Yamaguchi et al., $PbCO_3$ decomposes in air at 200 °C producing an intermediate with formula $PbCO_3{\cdot}2PbO$, then this compound decomposes to PbO at 310 °C [27]. These authors have reported the thermal decomposition of $PbCO_3$ at different CO_2 pressures; at 1 atm of CO_2 two intermediates were found with formula $PbCO_3{\cdot}PbO$ and $PbCO_3{\cdot}2PbO$. These intermediates decompose at 440 °C producing PbO as final product. When the decomposition was performed at pressures

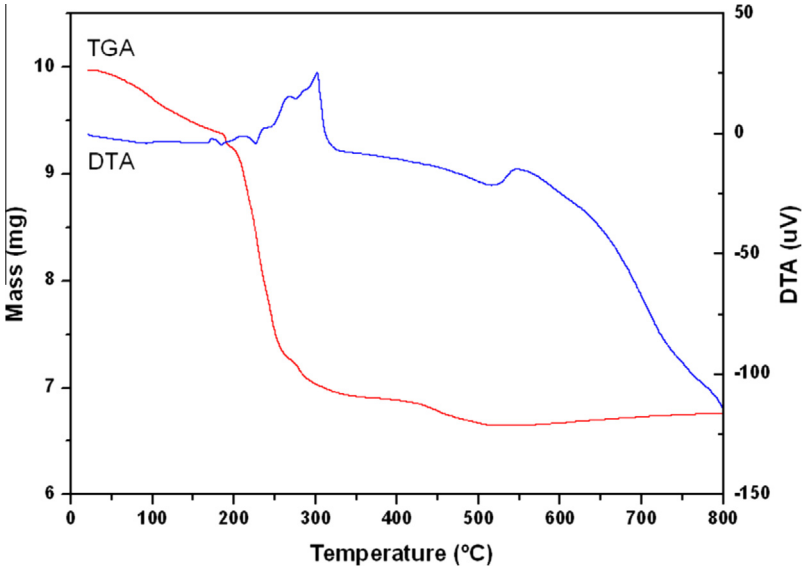

Fig. 1. TG and DT curves for $Pb[Mn(C_3H_2O_4)_2(H_2O)_2]$ in air.

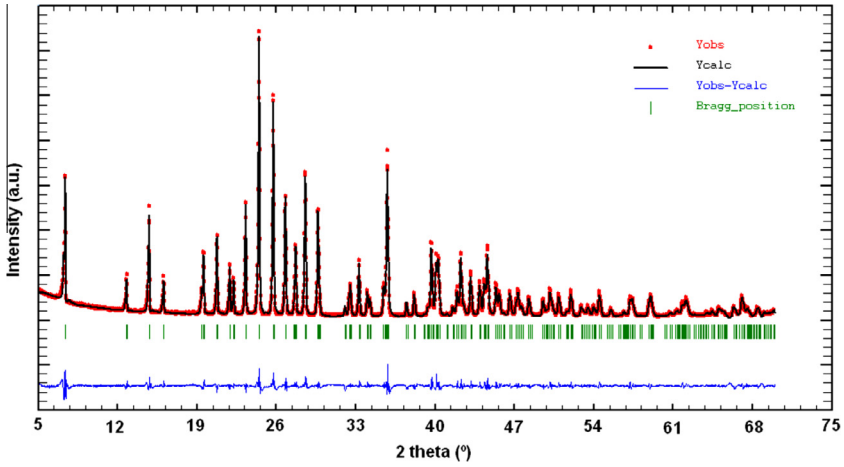

Fig. 2. PXRD pattern observed (red), calculated (black) and difference curve (blue) for the Le Bail refinement of $Pb[Mn(C_3H_2O_4)_2(H_2O)_2]$. (For interpretation of the references to color in this figure legend, the reader is referred to the web version of this article.)

higher than 4 atm of CO_2, three intermediates were found ($2PbCO_3{\cdot}PbO$, $PbCO_3{\cdot}PbO$, $PbCO_3{\cdot}2PbO$); these intermediates decompose at different temperatures producing PbO as final product [27]. In our conditions, CO_2 was produced by decarboxylation of the malonato ligand and the decomposition of $PbCO_3$ occurs at higher temperatures compared with the value reported by pure $PbCO_3$. The residues obtained from the thermal decomposition of the complex at 500 °C were MnO_2 and PbO. Similar results were obtained by different complexes containing malonato ligand and alkaline-earth metals such as $Sr[Mn(C_3H_2O_4)_2(H_2O)_4]$ and $Ba[Mn(C_3H_2O_4)_2(H_2O)_4]$ where the carbonates of the alkaline-earth are stable and decompose producing the corresponding mixed oxide as final product [9–10]. The thermal decomposition products were identified using PXRD data (see below). At temperatures higher than 600 °C the mass remains constant.

Structural characterization

Powder X-ray diffraction data

The PXRD pattern of $Pb[Mn(C_3H_2O_4)_2(H_2O)_2]$ refined by the Le Bail method is shown in Fig. 2. The pattern was indexed using the program TREOR [19] with the first 25 diffraction peaks of the pattern. A hexagonal unit cell was found with high figures of merit $M(25) = 115$ and $F(25) = 496$. From the extinction analysis two space groups were found to be possible according to the systematic absences: $P6_3cm$ and $P6_3/mcm$. After the Le Bail profile fitting we have concluded that the complex crystallizes in the hexagonal crystal system, space group $P6_3/mcm$ with cell parameters $a = b = 13.8366(7)$ Å, $c = 9.1454(1)$ Å, $\gamma = 120$ °, $V = 1516.3(1)$ Å^3.

Quantum chemical calculations

The molecular structure of the anion complex $[Mn(C_3H_2O_4)_2(H_2O)_2]^{2-}$ optimized using the B3LYP method with LANL2DZ basis sets for the Mn atom and 6-311G(d,p) basis sets for the non metal atoms is shown in Fig. S1. The calculated geometrical parameters are listed in Table 1. These parameters are in good agreement with the values reported by single crystal of related malonato complexes [1–6,28]. As can be seen in Fig. S1, the Mn(II) ion is six-coordinated in slightly distorted octahedral environment, two coordinated water molecules are located in apical positions and four oxygen atoms from two malonato ligands are located in the equatorial plane. The equatorial Mn–O bond lengths are somewhat

Table 1
Geometrical parameters calculated for the anion complex $[Mn(C_3H_2O_4)_2(H_2O)_2]^{2-}$ calculated at the B3LYP level with LANL2DZ basis set for the Mn atom and 6-311G(d,p) for non metallic atoms.

Parameter[a]	Calculated[b]	Experimental[c]
Mn–O(25) w	2.181	2.180
Mn–O(24) w	2.181	2.180
Mn–O(2)	2.167	2.117
Mn–O(3)	2.382	2.184
C(2)–C(4)	1.294	1.262
C(4)–C(6)	1.482	1.269
C(6)–C(9)	1.538	1.527
C(9)–O(3)	1.588	1.269
C=O (mean)	1.227	1.255
O(2)–Mn–O(3)	87.34	86.80
O(2)–Mn–O(25) w	90.25	88.90
O(2)–Mn–O(12)	81.38	93.20
O(11)–Mn–O(24) w	86.65	91.10
C(6)–C(4)–O(2)	123.43	123.07
C(4)–C(6)–O(3)	110.28	114.50
C(6)–C(9)–O(10)	113.22	117.79
C(6)–C(9)–O(3)	123.63	118.32

[a] Bond lengths in Å and bond angles in degrees. See Fig. S1 for atoms numbering.
[b] Calculated at B3LYP level with LANL2DZ basis set for the Mn atom and 6-311G(d,p) for non metallic atoms.
[c] Taken from Ref. [28] for the complex $(C_6H_8N_2H)_2[Mn(C_3H_2O_4)_2]\cdot 4H_2O$.

shorter than the apical ones (see Table 1), leading to an elongated distorted octahedral environment around Mn(II) ion. The values of C–C and C–O malonato bond distances and O–C–O bond angles agree well with those previously reported for other malonato-containing complexes [1–6,28]. The chelated malonato ring formed by the O(2)–C(4)–C(6)–C(9)–O(3) atoms has an envelope conformation in which only the methylene group is significantly displaced from the ring plane, while the other ring formed by the O(12)–C(15)–C(17)–C(13)–O(11) atoms is quite planar (see Fig. S1). The difference in the C(4)–C(6)–C(9), 125.6° and C(15)–C(17)–C(13), 119.3° angles could be explained on the basis of these linkages and the conformation of the ligands. In both malonato ligands, the average C=O bond distances and O–C–O angles are 1.227 Å and 122.6°, respectively.

Vibrational analysis

According to the general structural characteristics described above, it is evident that the internal vibrations of the title compound can be described by means of the following building units:

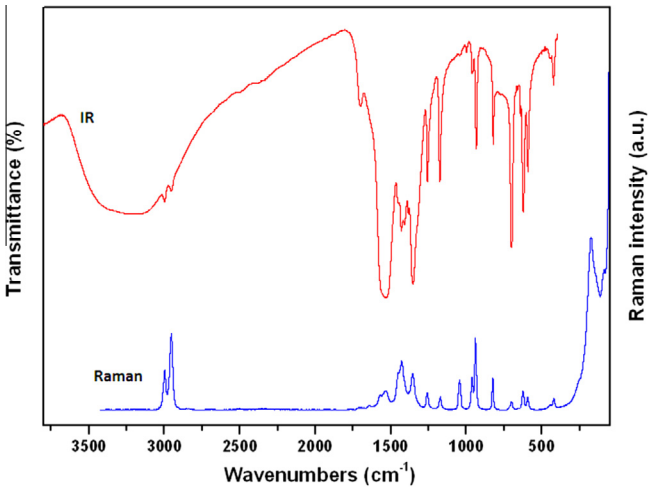

Fig. 3. IR and Raman spectra of the complex $Pb[Mn(C_3H_2O_4)_2(H_2O)_2]$ in solid state.

carboxylate groups, methylene groups and water molecules. The interpretations and assignment of the experimental bands of the IR and Raman spectra was made in comparison with those observed for malonic acid and related compounds containing the malonato ligand [1–6,28–30]. The experimental IR and Raman spectra of the solid complex $Pb[Mn(C_3H_2O_4)_2(H_2O)_2]$ measured at room temperature is shown in Fig. 3. The details of the IR and Raman spectra, together with a tentative assignment, are collected in Table 2.

Assignment of bands

Water modes. The presence of one kind of water molecules in the solids are evidenced by their IR characteristic vibration modes. In $Pb[Mn(C_3H_2O_4)_2(H_2O)_2]$, the frequency values of the O–H stretching vibration are lower than those expected for free water molecules. The broad band located between 3600 and 3000 cm^{-1} can be assigned to the ν(O–H) stretching vibrations suggesting that all of the water molecules are similar. The bands corresponding to the bending mode of H_2O (in the region 1650–1600 cm^{-1}) are overlapped with the bands corresponding to carboxylate groups. The librational modes of coordinated water (rocking, wagging and twisting), which usually present low intensity and are strongly overlapped with other modes, are difficult to identify. The band at 423 cm^{-1} in the IR spectrum is assigned to the M–OH_2 stretching vibration.

Carboxylate group modes. In malonic acid, the IR spectrum shows two strong absorption bands at 1740 and 1710 cm^{-1} assigned to the ν(C=O) stretching vibration [29]. The free malonato ion presents resonance between the two C–O bonds; in consequence the characteristic carbonyl absorption is replaced by two bands located in the frequency range 1610–1550 cm^{-1} and 1400–1350 cm^{-1} that could be assigned to the anti-symmetric and symmetric stretching vibration of the carboxylate group, respectively [30]. Generally, these bands appear as a doublet with a separation in the order of 20–40 cm^{-1}.

Table 2
Experimental frequencies (in cm^{-1}) and assignment of the fundamental vibrational modes of $Pb[Mn(C_3H_2O_4)_2(H_2O)_2]$.

Infrared (solid)[a]	Raman (solid)[b]	Assignment[c]
3600–3000 b	–	ν(O–H)
2998 w	2997 (23)	$\nu_a(CH_2)$
2955 vw	2954 (44)	$\nu_s(CH_2)$
1702 w	–	ν(C=O)
1562 vs	1571 (9)	ν_a(OCO)
1533 vs	1532 (11)	ν_a(OCO)
1453 w	1453 sh	$\delta(CH_2)$
1431 m	1428 (28)	$\delta(CH_2)$
1354 s	1356 (21)	ν_s(OCO)
1258 m	1260 (10)	$\omega(CH_2)$
1176 m	1173 (8)	ν_a C–C
–	1045 (17)	ν_s C–C
962 vw	963 (19)	$\rho(CH_2)$
934 m	941 (42)	$\rho(CH_2)$
822 m	825 (18)	δ(C–C)
702 s	702 (5)	δ(OCO)
642 w	–	γ(OCO)
624 m	625 (11)	δ(CCO)
592 m	594 (7)	δ(CCO)
423 w	421(7)	ν(M–O)
–	251 sh	ν(M–O)
–	175 (100)	ν(M–O)
–	87 (80)	ν(M–O)

[a] sh, shoulder; s, strong; w, weak; m, medium; v, very; b, broad.
[b] Relative band heights in parentheses.
[c] $\underline{\nu}$: stretching, δ: in-plane deformation, γ: out-of-plane deformation, ρ: rocking, ω: wagging, $\tau\omega$: twisting, τ: torsion modes.

The spectra of the complex $Pb[Mn(C_3H_2O_4)_2(H_2O)_2]$ are in agreement with the spectra of different malonato complexes [1–6,28–30]. The two bands located at 1562 and 1533 cm^{-1} in the IR spectrum (1571 and 1532 cm^{-1} in Raman) are assigned to the anti-symmetric stretching vibration of the carboxylate group. The band corresponding to the symmetric stretching vibration of the OCO group appears at 1354 cm^{-1} without splitting. In the Raman spectrum, this mode appears at 1356 cm^{-1}. The difference between the frequency values of anti-symmetric and symmetric stretching modes ($\Delta\nu$) is in the expected range for compounds having both chelating or chelating and bridging carboxylate groups [1–6,28–30]. The high value of $\Delta\nu = 208$ cm^{-1} confirms the bidentate coordination modes associated with the two independent carboxylate groups present in the title complex. The shoulder located at 1702 cm^{-1} in the IR spectrum could be attributed to the existence of C=O groups, which are not linked to any metal ions. Nevertheless, the appearance of a broad band in this region, probably due to the presence of hydrogen bonds between the water molecules and the carboxylate groups, hampers the assignment of free carboxylate groups in the IR spectrum.

The bands located at 702 cm^{-1} in the IR and Raman spectra are assigned to the bending mode of the carboxylate groups, δ(OCO). The band located at 642 cm^{-1} in the IR spectrum corresponds to the out of plane deformation of the OCO group [30].

C–C modes. The weak band located at 1176 cm^{-1} in the IR spectrum (1173 cm^{-1} in Raman) could be assigned to the ν_a(C–C) mode. The band at 1045 cm^{-1} in the Raman spectrum is assigned to the ν_s(C–C) stretching mode. The intense band located at 825 cm^{-1} in the Raman spectrum is attributed to the C–C bending mode [30].

Methylene group modes. The weak band observed in the IR spectrum at 2998 cm^{-1} (2997 cm^{-1} in Raman) is assigned to the anti-symmetric stretching mode of the CH_2 group. The intense band located at 2954 cm^{-1} in the Raman spectrum is assigned to the symmetric stretching vibration of this mode.

The two bands observed in the IR spectrum at 1453 and 1431 cm^{-1} are assigned to the bending modes of methylene consistent with the two bands at 1453 and 1428 cm^{-1} in the Raman spectrum.

The band corresponding to the wagging deformation mode is observed at 1258 cm^{-1} in the IR spectrum (1260 cm^{-1} in Raman) and the two intense bands located at 963 and 941 cm^{-1} in the Raman spectrum are assigned to the rocking mode. This assignment is in agreement with the reported by Schmelz et al. which have informed the band corresponding to the wagging mode at 1290 cm^{-1} and the band assigned to the rocking mode at 938 cm^{-1} for $Na_2[Cu(C_3H_2O_4)_2(H_2O)_2]$ complex [30].

Skeletal modes. The two bands observed in the IR spectrum at 624 and 592 cm^{-1} (625 and 594 cm^{-1} in Raman) are assigned to the CCO bending mode. The bands located at 251, 175 and 87 cm^{-1} in the Raman spectrum could be assigned to the M–O stretching modes [29–30].

Thermal treatments of $Pb[Mn(C_3H_2O_4)_2(H_2O)_2]$ at different temperatures

Taking into account the previous analysis (TG and DT), thermal treatments of $Pb[Mn(C_3H_2O_4)_2(H_2O)_2]$ in air at different temperatures were carried out. The quantitative composition of the residues at different temperatures was determined using X'Pert Highscore Program (version 2.1b). The PXRD patterns of the residues obtained by heating of $Pb[Mn(C_3H_2O_4)_2(H_2O)_2]$ in air at different temperatures for 6 h are shown in Fig. 4.

When the complex was heated at 550 °C, some peaks attributed to PbO massicot (PDF #072-0093), PbO litharge (PDF #085-1288), Pb_3O_4 (PDF #076-1799) and Pb_2MnO_4 (PDF #036-0844) were observed. When the complex was heated at 600 and 700 °C, the PXRD pattern shows only lines corresponding to PbO massicot and litharge and Pb_2MnO_4. Kimber et al. have reported the synthesis of the compound Pb_2MnO_4 by the ceramic method using PbO and Mn_2O_3 as reagents in air at 730 °C for one week [31], however this compound was obtained as a pure phase using the Pechini method at 700 °C for 10 h in air [32]. The mixed oxide Pb_2MnO_4 crystallizes in the space group $P\text{-}42_1c$ and it exhibits a specific structure similar to Pb_3O_4 (Pb_2PbO_4) [31]. The structure consists of zig-zag chains of edge-sharing MnO_6 octahedra parallel to the *c* axis that delimit one-dimensional tunnels into which the Pb^{2+} cations project and have an off-center coordination by oxygen that may be attributed to a $6s^2$ lone pair [31]. Halasyamani et al. have reported that Pb_2MnO_4 allows piezoelectricity [33]. As Pb_2MnO_4 also contains magnetic $3d^3$ Mn^{4+} ions, it is likely that a long range ordered spin state is formed at low temperatures. This ordering was determined by Kimber et al. by magnetization and neutron diffraction measurements [31]. Pb_2MnO_4 is an excellent candidate to be a multipiezo (coupled magnetization and electrical polarization under mechanical stress) material.

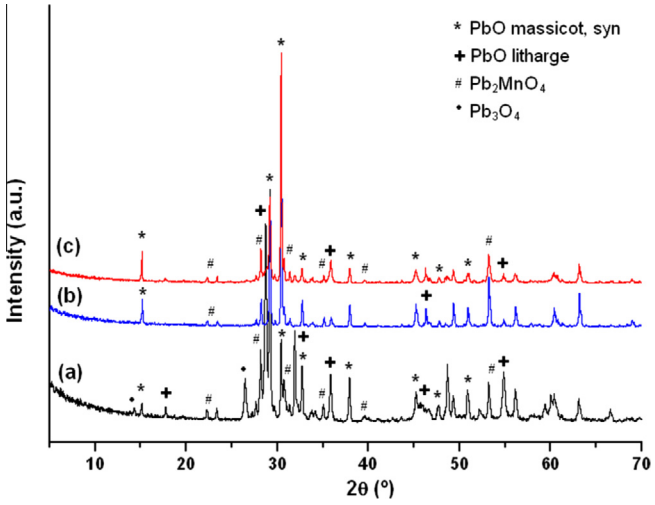

Fig. 4. PXRD patterns of residues obtained by thermal treatments of $Pb[Mn(C_3H_2O_4)_2(H_2O)_2]$ at (a) 550 °C, (b) 600 °C and (c) 700 °C.

Conclusions

The metallo-organic complex $Pb[Mn(C_3H_2O_4)_2(H_2O)_2]$ was synthesized for the first time and characterized by powder XRD, IR and Raman spectroscopy. Quantum chemical calculations of the complex anion $[Mn(C_3H_2O_4)_2(H_2O)_2]^{2-}$ were performed in order to understand the structural characteristics of the metal complex. The cell parameters of $Pb[Mn(C_3H_2O_4)_2(H_2O)_2]$ were obtained by autoindexing the PXRD pattern and refined using the Le Bail method. The complex crystallizes in the hexagonal crystal system in the space group $P6_3/mcm$ with cell parameters $a = b = 13.8366(7)$ Å, $c = 9.1454(1)$ Å, $\gamma = 120°$. The DFT calculated geometry of the $[Mn(C_3H_2O_4)_2(H_2O)_2]^{2-}$ structure is very close to the experimental data reported for similar systems. The IR and Raman spectra indicate that only one type of water molecules are present in the structure as was deduced by thermal analysis. All the bands corresponding to the malonato ligand were assigned according to the calculations and related molecules. The thermal decomposition of the $Pb[Mn(C_3H_2O_4)_2(H_2O)_2]$ complex in air was

studied using TG/DT analysis. It decomposes in three steps. The first one corresponds to the elimination of two water molecules. The two following steps are associated to the decarboxylation of the ligand to produce MnO_2 and PbO as final products. The thermal treatments of $Pb[Mn(C_3H_2O_4)_2(H_2O)_2]$ at 700 °C produces PbO massicot and litarge and the mixed oxide Pb_2MnO_4. These results demonstrated that the decomposition of the metallo-organic complex is better to prepare mixed oxides at low temperature than ceramic methods.

Acknowledgments

D.M.G. thanks CONICET for fellowships. M.I.G. thanks CIUNT for financial support, Project 26D/428. R.E.C. thanks support from CONICET – Argentina (PIP #11220090100995) and SECyT-UNC (Project 162/12).

Appendix A. Supplementary data

Supplementary data associated with this article can be found, in the online version, at http://dx.doi.org/10.1016/j.saa.2015.01.057.

References

[1] F.S. Delgado, M. Hernández Molina, J. Sanchiz, C. Ruiz Pérez, Y. Rodriguez Martín, T. López, F. Lloret, M. Julve, CrystEngComm 6 (2004) 106.
[2] C. Ruiz Pérez, Y. Rodriguez Martín, M. Hernández Molina, F.S. Delgado, J. Pasán, J. Sanchiz, F. Lloret, M. Julve, Polyhedron 22 (2003) 2111.
[3] F.S. Delgado, J. Sanchiz, C. Ruiz Pérez, F. Lloret, M. Julve, CrystEngComm 5 (2003) 280.
[4] R.P. Scaringe, W.E. Hatfield, D.J. Hodgson, Inorg. Chem. 16 (1977) 1600.
[5] D. Chattopadhyay, S.K. Chattopadhyay, P.R. Lowe, C. Schwalke, S.K. Mazumber, A. Rana, S. Ghosh, J. Chem. Soc., Dalton Trans. (1993) 913.
[6] S.H. Saadeh, K.L. Trojan, J.W. Kampf, W.E. Hatfield, V.L. Peroraro, Inorg. Chem. 32 (1993) 3034.
[7] I. Gil de Muro, M. Insausti, L. Lezama, T. Rojo, J. Solid State Chem. 178 (2005) 1712.
[8] I. Gil de Muro, M. Insausti, L. Lezama, T. Rojo, J. Solid State Chem. 178 (2005) 928.
[9] I. Gil de Muro, M. Insausti, L. Lezama, J.L. Pizarro, M.I. Arriortua, T. Rojo, Eur. J. Inorg. Chem. (1999) 935.
[10] I. Gil de Muro, F.A. Mautner, M. Insausti, L. Lezama, M.I. Arriortua, T. Rojo, Inorg. Chem. 37 (1999) 3243.
[11] I. Gil de Muro, L. Lezama, M. Insausti, T. Rojo, Polyhedron 23 (2004) 929.
[12] D.M. Gil, M.C. Navarro, M.C. Lagarrigue, J. Guimpel, R.E. Carbonio, M.I. Gómez, J. Mol. Struct. 1003 (2011) 129.
[13] M.C. Navarro, E.V. Pannunzio-Miner, S. Pagola, M.I. Gómez, R.E. Carbonio, J. Solid State Chem. 178 (2005) 847.
[14] D.M. Gil, M.C. Navarro, M.C. Lagarrigue, J. Guimpel, R.E. Carbonio, M.I. Gómez, J. Therm. Anal. Calorim. 103 (3) (2011) 889.
[15] D.M. Gil, R.E. Carbonio, M.I. Gómez, J. Chil. Chem. Soc. 55 (2010) 189.
[16] D.M. Gil, M. Avila, E. Reguera, S. Pagola, M.I. Gomez, R.E. Carbonio, Polyhedron 33 (2012) 450.
[17] D.M. Gil, R.E. Carbonio, M.I. Gómez, J. Mol. Struct. 1041 (2013) 23.
[18] D.M. Gil, G. Nieva, D.G. Franco, M.I. Gómez, R.E. Carbonio, Mater. Chem. Phys. 141 (2013) 355.
[19] P.E. Werner, L. Eriksson, M. Westdahl, J. Appl. Crystallogr. 18 (1985) 367.
[20] A. Le Bail, H. Duroy, J.L. Fourquet, Mater. Res. Bull. 23 (1988) 447.
[21] J. Rodriguez-Carbajal, Physica B 192 (1993) 55.
[22] L.W. Finger, D.E. Cox, A.P. Jephcoat, J. Appl. Crystallogr. 27 (1994) 892.
[23] A.D. Becke, J. Chem. Phys. 98 (1993) 5648.
[24] C. Lee, W. Yang, R.G. Parr, Phys. Rev. B 37 (1988) 785.
[25] A.D. Becke, Phys. Rev. A 38 (1988) 3098.
[26] M.J. Frisch, G.W. Trucks, H.B. Schlegel, G.E. Scuseria, M.A. Robb, J.R. Cheeseman, J.A. Montgomery Jr., T. Vreven, K.N. Kudin, J.C. Burant, J.M. Millam, S.S. Iyengar, J. Tomasi, V. Barone, B. Mennucci, M. Cossi, G. Scalmani, N. Rega, G.A. Petersson, H. Nakatsuji, M. Hada, M. Ehara, K. Toyota, R. Fukuda, J. Hasegawa, M. Ishida, T. Nakajima, Y. Honda, O. Kitao, H. Nakai, M. Klene, X. Li, J.E. Knox, H.P. Hratchian, J.B. Cross, C. Adamo, J. Jaramillo, R. Gomperts, R.E. Stratmann, O. Yazyev, A.J. Austin, R. Cammi, C. Pomelli, J.W. Ochterski, P.Y. Ayala, K. Morokuma, G.A. Voth, P. Salvador, J.J. Dannenberg, V.G. Zakrzewski, S. Dapprich, A.D. Daniels, M.C. Strain, O. Farkas, D.K. Malick, A.D. Rabuck, K. Raghavachari, J.B. Foresman, J.V. Ortiz, Q. Cui, A.G. Baboul, S. Clifford, J. Cioslowski, B.B. Stefanov, G. Liu, A. Liashenko, P. Piskorz, I. Komaromi, R.L. Martin, D.J. Fox, T. Keith, M.A. Al-Laham, C.Y. Peng, A. Nanayakkara, M. Challacombe, P.M.W. Gill, B. Johnson, W. Chen, M.W. Wong, C. González, J.A. Pople, Gaussian 03, Revision C.02, Gaussian Inc., Wallingford, CT, 2004.
[27] J. Yamaguchi, Y. Sawada, O. Sakurai, K. Uematsu, N. Mizutani, M. Kato, Thermochim. Acta 35 (1980) 307.
[28] S.R. Choudhury, B. Dey, S. Das, A. Robertazzi, A.D. Jana, C.Y. Chen, H.M. Lee, P. Gamez, S. Mukhopadhyay, Dalton Trans. (2009) 7617.
[29] K. Nakamoto, Infrared and Raman Spectra of Inorganic and Coordination Compounds, fifth ed., Wiley-Interscience, New York, 1997.
[30] M.J. Schmelz, I. Nakagawa, S.I. Mizushima, J.V. Quagliano, J. Am. Chem. Soc. 81 (1959) 287.
[31] S.A.J. Kimber, J.P. Attfield, J. Mater. Chem. 17 (2007) 4885.
[32] H. Serier-Brault, M. Jansen, Solid State Sci. 13 (2011) 326.
[33] P.S. Halasyamani, K.R. Poeppelmeier, Chem. Mater. 10 (1998) 2753.